Nucleolus and c-Myc: potential targets of cardenolide-mediated antitumor activity

Tatjana Mijatovic,[1] Nancy De Nève,[1] Philippe Gailly,[2] Véronique Mathieu,[3] Benjamin Haibe-Kains,[4,5] Gianluca Bontempi,[4] Javier Lapeira,[6] Christine Decaestecker,[3] Vincenzo Facchini,[1] and Robert Kiss[3]

[1]Unibioscreen SA; [2]Department of Physiology and Pharmacology, Catholic University of Louvain; [3]Laboratory of Toxicology, Institute of Pharmacy; [4]Machine Learning Group, Department of Computer Science, Free University of Brussels; [5]MicroArray Unit, Jules Bordet Institute, Brussels, Belgium; and [6]University of Rochester, New York, New York

Abstract

The use of cardenolides like ouabain, digitoxin, or oleandrin has been reported previously many times as a means of potentially combating human refractory prostate cancer by inducing apoptosis through an increase in intracellular calcium concentrations. The aims of the current study were to investigate if part of the antitumor effects mediated by cardenolides concerned disorganization of nucleolar structure and whether this was further associated with a marked decrease in c-Myc expression. Accordingly, the antitumor activity of a novel hemisynthetic cardenolide [1*R*,3a*S*,3b*R*,5a*S*,6a*R*,7a*S*,9*R*,12a*R*,13a*R*,15a*R*]-3a,11a-dihydroxy-13a-(hydroxymethyl)-9,15a-dimethyl-1-(5-oxo-2,5-dihydrofuran-3-yl)icosahydro-1*H*,4′*H*-spiro[cyclopenta [7,8] phenanthro[2,3-*b*]pyrano[3,2-*e*][1,4]dioxine-11,2′-[1,3] thiazolidin]-4′-one (UNBS1450)] was compared with that of classic cardenolides and reference anticancer agents in prostate cancer cell lines *in vitro* and *in vivo* following s.c. and orthotopic prostate cancer cell grafting into mice. The present study indicates that UNBS1450 markedly decreases the *in vitro* viability/proliferation of human prostate cancer cell lines but not of normal cells. The induced effects are not linked to an increase in intracellular calcium concentrations and subsequent induction of apoptosis. Rather, they appear to relate to the compound's capacity to disorganize nucleolar structure and function (through an impairment of cyclin-dependent kinase and c-Myc expression and related signaling pathways; paralleled by the disorganization of cancer cell-specific perinucleolar bodies as revealed by disruption of Sam68). This nonapoptotic cancer cell death mediated by severe nucleolar targeting and down-regulation of c-Myc expression is a completely new cardenolide-induced mechanism of antitumor action. [Mol Cancer Ther 2008; 7(5):1285–96]

Introduction

Apart from skin cancer, prostate cancer is the most frequently diagnosed and the second leading cause of death as a result of cancer in men in the United States (1, 2). The use of cardiotonic steroids like ouabain, digitoxin, or oleandrin has been reported previously many times as a means of potentially combating human refractory prostate cancer (3–6). Cardenolides belong to a broader chemical class known as cardiac glycosides, whose receptor is the sodium pump, Na^+/K^+-ATPase (7, 8). The sodium pump is a membrane-bound protein (an oligomer composed of stoichiometric amounts of two major polypeptides, the α- and β-subunits) that establishes and maintains the high internal K^+ and low internal Na^+ cellular concentrations typical of most animal cells (9). In addition to its function as an ion transporter, the sodium pump acts as a signal transducing molecule that transmits the effects of cardenolides into the cell (7, 8). Cross-talk among the affected pathways eventually results in changes in the expression of several genes (8). Inhibition of Na^+/K^+-ATPase leads to cell type-specific modulation of cell proliferation and survival (8).

Chemical modifications of 2″-oxovoruscharin (a novel cardenolide that was isolated from the African plant *Calotropis procera*) based on an understanding of the structure-activity relationship within the series has led to the identification of a new cardenolide: (1*R*,3a*S*,3b*R*,5a*S*,6a*R*,7a*S*,9*R*,12a*R*,13a*R*,15a*R*)-3a,11a-dihydroxy-13a-(hydroxymethyl)-9,15a-dimethyl-1-(5-oxo-2,5-dihydrofuran-3-yl)icosahydro-1*H*,4′*H*-spiro[cyclopenta [7,8]phenanthro[2,3-*b*]pyrano[3,2-*e*][1,4]dioxine-11,2′-[1,3]thiazolidin]-4′-one (UNBS1450; Fig. 1A; ref. 10). This molecule has a relatively different structure compared with that of known cardenolides, with a novel sugar moiety double linked to the steroid backbone and *trans*-positioning as opposed to *cis*-positioning of rings A and B of the steroid backbone. These differences may contribute to the compound's unique mechanism of action following its

Received 10/29/07; revised 2/19/08; accepted 3/3/08.

Grant support: Fonds Yvonne Boël (Brussels, Belgium) and Région de Bruxelles-Capitale (Brussels, Belgium). T. Mijatovic and N. De Nève are employees of Unibioscreen SA, Brussels, Belgium. V. Mathieu is the holder of a Grant Télévie from the Fonds National de la Recherche Scientifique (Belgium). C. Decaestecker is a Senior Research Associate and R. Kiss is a Director of Research with the Fonds National de la Recherche Scientifique.

The costs of publication of this article were defrayed in part by the payment of page charges. This article must therefore be hereby marked *advertisement* in accordance with 18 U.S.C. Section 1734 solely to indicate this fact.

Requests for reprints: Robert Kiss, Laboratory of Toxicology, Institute of Pharmacy, Free University of Brussels, Campus de la Plaine CP205/1, Boulevard du Triomphe, 1050 Brussels, Belgium. Phone: 32-477-62-20-83; Fax: 32-2-332-53-35. E-mail: rkiss@ulb.ac.be

doi:10.1158/1535-7163.MCT-07-2241

interaction with the sodium pump (11–14) and, more specifically, may have an effect on the nucleolus (the present study). Using computer-assisted phase-contrast microscopy (15, 16) as a morphology-based screening approach, we have observed that UNBS1450 markedly modifies the shape and organization of the nucleolus. The nucleolus is a nuclear domain and the site of ribosome biogenesis that is crucial to cell survival (17). Nucleoli are generally composed of three morphologically distinct subdomains: the fibrillar centers (the sites of transcription and processing of rRNA; revealed by fibrillarin staining), the dense fibrillar component [the regions that are thought to be the interphase equivalent of nucleolar-organizing regions of chromosomes; revealed by upstream binding factor (UBF) staining], and finally the granular component (18). Recent evidence that several tumor suppressors and oncoproteins, such as p53, MDM2, p19ARF, IRS, nucleophosmin, and MYC, are sequestered in the nucleoli of tumor cells suggests a cancer-related role for nucleoli that goes beyond protein synthesis (19). Compounds that selectively target perturbations in the organization of nucleolar machinery could thus represent potentially a new means of anticancer therapy.

The aims of this study were thus to investigate nucleolar targeting in relation to the anticancer activity against human prostate cancer cells of the new hemisynthetic cardenolide UNBS1450, which belongs to structurally different class compared with digitalis-like compounds (10).

Materials and Methods

Compounds

Drugs were purchased as follows: ouabain (Acros Organics), digitoxin (Acros Organics), digoxin (Sigma), Taxol (paclitaxel; Bristol-Myers Squibb), irinotecan (Campto; Aventis), 7-ethyl-10-hydroxycamptothecin (Aventis), oxaliplatin (Inter-Chemical), etoposide (Bristol-Myers Squibb), and mitoxantrone (Sigma). As detailed elsewhere (10), 2″-oxovoruscharin (UNBS1244) was chemically extracted from the bark of the African plant *C. procera*; specimens of which were provided by Prof. Pierre Guissou (Laboratory of Toxicology, University of Ouagadougou, Burkina Faso). UNBS1450 was obtained from the UNBS1244 by means of hemisynthesis in Unibioscreen laboratory facilities (10).

Cell Lines

The human prostate cancer cell lines LNCaP (CRL-1740), PC-3 (CRL-1435), and DU145 (HTB-81) and human normal lung WI-38 (CCL-75) and skin WS-1 (CRL-1502) fibroblast cell lines were obtained from the American Type Culture Collection and were maintained as described in refs. 10, 12.

In vitro Overall Growth Determination

Overall cell growth was assessed by means of the colorimetric 3-[4,5-dimethylthiazol-2yl]-diphenyltetrazolium bromide (MTT; Sigma) assay as detailed elsewhere (10–14). The cells were incubated for 72 h in the presence or the absence (controls) of the various drugs. Drug concentrations ranged between 10^{-9} and 10^{-5} mol/L (with semilog concentration increases). Experiments were carried out in sextuplicate.

In vivo S.c. and Orthotopic Grafting of PC-3 Human Prostate Cancer Cells onto Mice

S.c. xenografts were realized by injecting 2.5×10^6 human PC-3 cells onto the left flanks of 8-week-old male NMRI *nu/nu* mice (21-23 g; BioServices). For ethical reasons, the endpoint in these experiments was the sacrifice of all s.c. PC-3 xenograft-bearing mice when the mean tumor size had reached 500 mm^2 in the control group. Tumor size was measured twice weekly by means of calipers and expressed as an area (mm^2) by multiplying the two greatest perpendicular diameters. On this basis, the potential drug-induced inhibition of tumor growth was evaluated. Orthotopic xenografts were obtained by injecting 2.5×10^6 human PC-3 cells into the prostate of 8-week-old male NMRI *nu/nu* mice. All grafts were done under anesthesia [saline (Rompun; Bayer)/Imalgene (Merial), 5:1:1 by volume]. In the orthotopic PC-3 experiment, the key assessment was the determination of mouse survival times. For ethical reasons, animals were euthanized when 20% of body weight had been lost compared with that determined at the time of tumor grafting. Autopsies and histology were done on each mouse to confirm tumor development. In each experiment, 100% tumor development was obtained following PC-3 grafting. All *in vivo* experiments described in the current study were done based on authorization no. LA1230509 of the Animal Ethics Committee of the Belgian Federal Department of Health, Nutritional Safety and the Environment.

Total RNA Extraction

Total RNA was extracted using the TRIzol isolation reagent (Life Technologies) according to the manufacturer's instructions. The RNA extracted was treated with DNase I (Life Technologies) to eliminate any remaining genomic DNA. The quality and integrity of the extracted RNA were assessed by both BioAnalyzer 2100 (Agilent) and gel electrophoresis.

Standard Reverse Transcription-PCR Analysis

All reverse transcription and PCR were carried out in a thermal cycler (Thermocycler; Westburg). The purification of the cDNAs produced was carried out using the High Pure PCR Product Purification Kit (Roche Diagnostics) in accordance with the manufacturer's instructions. The integrity of the cDNA was confirmed by an analysis of β-actin gene expression based on a 25-cycle PCR analysis in a total volume of 50 μL with 20 ng loaded cDNA. All of the PCR analyses were done based on the same quantity of purified cDNA (total amount, 20 ng). The products amplified by means of the standard semiquantitative PCR (24-36 cycles with two-step cycle increases) were resolved by gel electrophoresis in 1.2% agarose TBE gels. The primers used for c-Myc PCR analyses (forward 5′-attctctgctctcctcga-3′ and reverse 5′-ccgttttagctcgttcct-3′) were provided by Invitrogen and selected using the HYBSIMULATOR software (Advanced Gene Computing Technology).

Genomic Analysis

Full genome-wide analyses were done at the VIB Microarray Facility (UZ Gasthuisberg, Catholic University of Leuven) using the Affymetrix Human Genome U133 set Plus 2.0. Each experimental condition was assessed in independent triplicates.

Microarray Data Analyses

In addition to *R*, an open-source software environment for statistical computing (20), a set of functions called *BioConductor* (21), was used for the analysis and comprehension of the genomic data. The quality controls in the Affymetrix microarray experiments were done with the *Simpleaffy* package (22) and agreed with the Affymetrix guidelines. The background correction, expression quantification, and normalization were done using *Robust Multichip Analysis* (23). To select differentially expressed genes between two experimental conditions, the probes were first identified for which no overlap occurred between intervals in the expression values obtained for each condition. The fold change between two experimental conditions was computed for each of these probes (without any value overlap) as the ratio between the two nearest un-log expression values observed for the two different conditions (that is, the ratio closest to 1 between any two values from the two different conditions). Probes for which these ratios were >2.0 or <0.50 were then selected. The annotations of the genes finally selected in this way were retrieved from the Affymetrix Web site through the *BioConductor* package *hgu133plus2*.

Flow Cytometry Analyses for the Determination of Reactive Oxygen Species Production

Reactive oxygen species (ROS) production was determined using 2′,7′-dichlorodihydrofluorescein diacetate (Fluka-Sigma). After PC-3 cells were treated with UNBS1450 at 10 and 100 nmol/L, they were loaded for 1 h with 2′,7′-dichlorodihydrofluorescein diacetate (20 μmol/L; as indicated in ref. 24) in RPMI 1640 without phenol red. Ten thousand individual data points were collected for each sample using a Becton Dickinson FACScan flow cytometer. Each experimental condition was evaluated in triplicate.

Flow Cytometry Analyses for Determining Apoptotic-Related Versus Nonapoptotic-Related Cell Death

Flow cytometry analyses of apoptotic-related versus nonapoptotic-related cell death were done according to the experimental protocol detailed previously in ref. 11. Each experiment was carried out in triplicate.

Western Blotting Analyses

Cell extracts were prepared by the lysis of subconfluent PC-3 cells directly in boiling lysis buffer [10 mmol/L Tris (pH 7.4), 1 mmol/L Na_3O_4V, 1% SDS (pH 7.4)]. Extracted proteins (40 μg; evaluated by the BCA protein assay; Pierce, Perbio Science) were loaded onto a denaturing polyacrylamide gel. Western blots were done as detailed in refs. 11, 12 and pertinent proteins were detected using primary antibodies provided by (*a*) CST Technologies: Rb (1:2,000), pRb (1:1,000), cyclin-dependent kinase 1 (CDK1; 1:1,000), phospho-CDK substrates (1:500), histone H3 (1:1,000; used as a loading control); (*b*) Abcam: fibrillarin (1:250), tubulin (1:3,000; used as a loading control); (*c*) BD Biosciences: poly (ADP-ribose) polymerase (1:250), caspase-3 (1:250), caspase-9 (1:250); and (*d*) Santa Cruz (Tebu Bio): UBF (1:200), c-Myc (1:400). Quantification of Western blots was done using a Fuji BASS5000 scanner and AIDA image analyzer software (Raytest Benelux).

Immunofluorescence Analyses

Immunofluorescence analyses were done as detailed in refs. 13, 14 with pertinent antibodies obtained as follows: fibrillarin from Abcam, c-Myc, UBF, and Sam68 from Santa Cruz (Tebu Bio). The Syto RNASelect (Molecular Probes, Invitrogen) green fluorescent cell stain, a cell-permeant nucleic acid stain that is selective for RNA, was used according to manufacturer's instructions to assess the UNBS1450-mediated effect on RNA accumulation in nucleoli. Phallacidin-conjugated with Alexa Fluor 488 fluorochrome (Molecular Probes) was used to label the fibrillar actin and Alexa Fluor 594–conjugated DNase I (Molecular Probes) to stain the globular actin. Fluorescence was visualized by a computer-assisted Olympus AX70 microscope (Omnilabo) equipped with a Megaview2 digital camera and analySIS software (Soft Imaging System).

Determination of Phospho-Rb Expression Levels Using an ELISA Assay

Phospho-Rb expression was determined using the specific human phospho-Rb ELISA assay (Sigma) according to instructions provided in the user manual. Roscovitine (75 μmol/L) was used as the positive control in the assay. Each experimental condition was evaluated in triplicate.

Intracellular Calcium Measurements

Cells were cultured to 30% to 50% confluence on glass coverslips to quantify $[Ca^{2+}]_i$. Thereafter, $[Ca^{2+}]_i$ measurements were done using Fura-2-AM as described previously (14).

Results

UNBS1450-Induced Marked *In vitro* Antiproliferative Activity in PC-3 Cells

UNBS1450 (Fig. 1A) displayed marked antiproliferative effects on refractory human prostate cancer PC-3 cells. This apoptosis-resistant cell line (p53 null and PTEN deleted) was chosen intentionally given that apoptosis resistance is the major problem in anticancer therapy and to show that UNBS1450 uses other pathways to elicit its anticancer activity. Figure 1B shows that although UNBS1450 displayed similar activity to Taxol it presented higher antiproliferative activity than other cardiac glycosides and cytotoxic agents (including mitoxantrone).

UNBS1450 Displays Significant Antitumor Effects *In vivo* in both Noninvasive S.c. and Highly Invasive Orthotopic PC-3 Models

UNBS1450 at 5 or 10 mg/kg i.p. (five injections per week for 3 consecutive weeks; starting on the 14th day post-tumor graft) notably decreased the growth rates of s.c. PC-3 tumors (Fig. 1C). In the orthotopic model, mitoxantrone at dose levels up to 5 mg/kg i.p. (three injections per week for

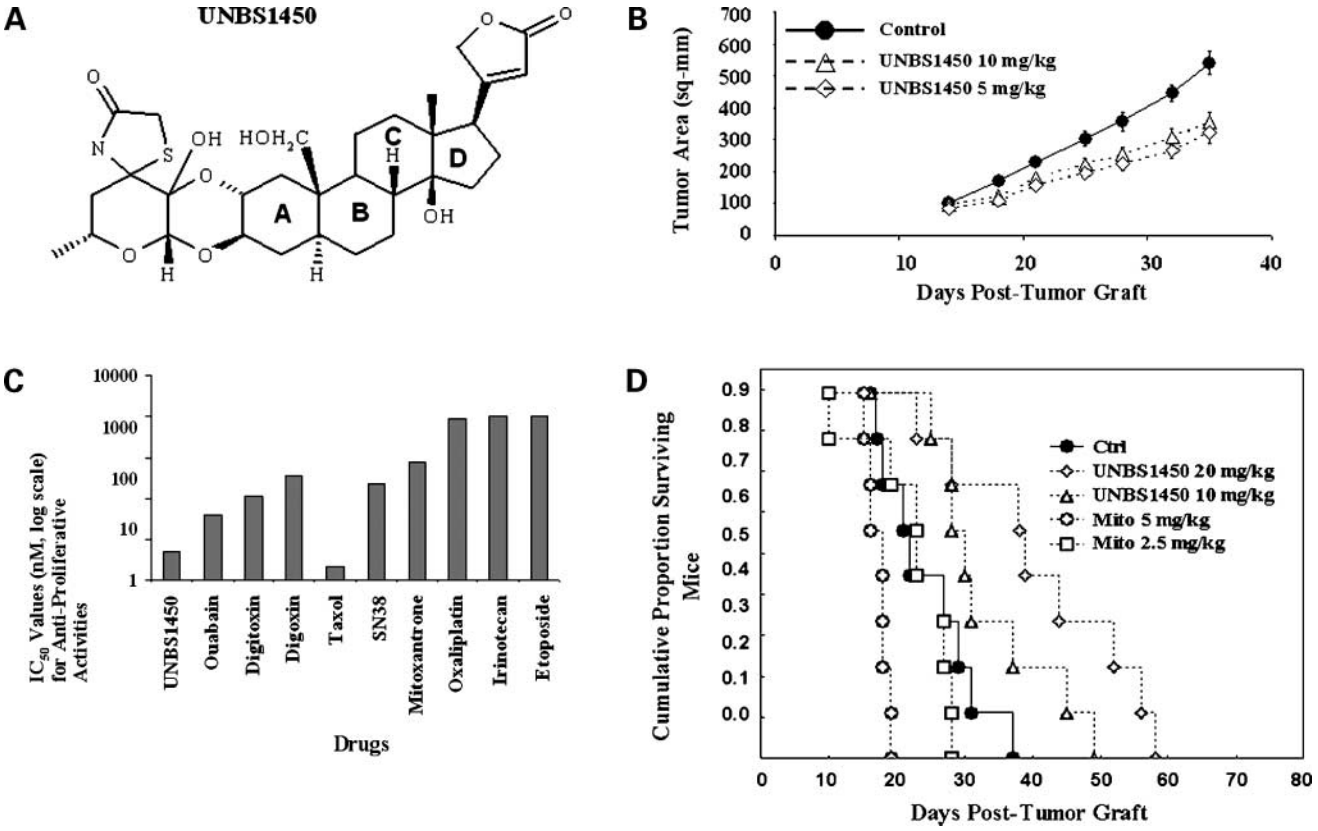

Figure 1. UNBS1450 antiproliferative activity. **A,** chemical structure of UNBS1450. **B,** *in vitro* antiproliferative effects of four cardiac glycosides/cardenolides (UNBS1450, ouabain, digitoxin, and digoxin) against the human PC-3 prostate cancer cell line in comparison with six anticancer drugs, Taxol, irinotecan, 7-ethyl-10-hydroxycamptothecin (the active metabolite of irinotecan), mitoxantrone, oxaliplatin, and etoposide. The results are presented as IC_{50} values (*Y axis,* logarithmic values) representing the concentrations at which each compound reduced the overall growth rate of the cell line by 50% after 3 d of treatment. Antiproliferative effects were evaluated by means of the MTT colorimetric assay. The drugs were assayed at nine distinct concentrations ranging from 10^{-9} to 10^{-5} mol/L involving semilog concentration increases with each concentration analyzed six times. **C** and **D,** *in vivo* UNBS1450-mediated antitumor activity. UNBS1450-mediated effects on the tumor growth rates of PC-3 s.c. xenografts (**C**) as well as on the survival periods of PC-3 orthotopic xenograft-bearing mice (**D**). In s.c. xenografts (**C**), UNBS1450 was evaluated i.p. (five injections per week for 3 wk) at 5 and 10 mg/kg. *Black circles,* control mice that received vehicle alone. Each group was composed of seven mice. In orthotopic xenografts (**D**), mitoxantrone (*Mito*) was evaluated i.p. at 1.25 and 0.63 mg/kg (three injections per week for 4 wk) or at 5 and 2.5 mg/kg (three injections per week for 3 wk) UNBS1450 was evaluated i.p. at 20 and 10 mg/kg (five injections per week for 6 wk). *Black circles,* control mice (*Ct*) that received vehicle alone. Each group was composed of nine mice.

3 or 4 weeks) did not significantly increase the survival of PC-3 xenograft-bearing mice (Fig. 1D). In sharp contrast, UNBS1450 at 10 and 20 mg/kg i.p. (five injections per week for 6 weeks) markedly increased the survival (by 36% and 77%, respectively) of PC-3 orthotopic xenograft-bearing mice.

Antiproliferative Effects of UNBS1450 in PC-3 Cells Do Not Relate to Induction of Apoptosis and Are Not Associated with a Rise in $[Ca^{2+}]_i$

UNBS1450 only slightly modified PC-3 cell cycle kinetics at 10 nmol/L (data not shown), a concentration corresponding to its antiproliferative IC_{50} in this cell line (Fig. 1A). At 100 nmol/L, UNBS1450 induced marked cell death (Fig. 2A), which precluded a reliable analysis of cell cycle kinetics. The present data indicate that UNBS1450 did not induce apoptosis (as revealed by flow cytometry analyses involving propidium iodide and Annexin V staining; Fig. 2A) in the PC-3 cell line in the concentration range (10-1,000 nmol/L) at which it markedly decreased global cell growth (Fig. 1B). This result was further corroborated by the inability of UNBS1450 treatment to induce poly (ADP-ribose) polymerase cleavage (at a drug concentration of 100 nmol/L; Fig. 2, *Ba*) or to activate caspase-3 (at 10-1,000 nmol/L; Fig. 2, *Bb*) and caspase-9 (at 10-1,000 nmol/L; Fig. 2, *Bc*) as revealed by Western blotting analyses. The induction of apoptosis by cardiac glycosides in human prostate cancer cells is linked to an increase in $[Ca^{2+}]_i$ (3, 4, 6). UNBS1450 did not increase $[Ca^{2+}]_i$ in PC-3 cells at 10 nmol/L (data not shown) and 100 nmol/L (Fig. 2C), that is, concentrations that markedly decreased the global growth of PC-3 cells (Fig. 1B) by inducing nonapoptotic cell death (Fig. 2A and B). ROS induction by several cardenolides is well documented and correlates with a loss in cell viability, proliferation, and defense mechanisms (5, 25). As shown in Fig. 2D, a marked time- and concentration-dependent ROS increase was shown

following UNBS1450 treatment (10 and 100 nmol/L). The inability of UNBS1450 to induce apoptosis has been evidenced in other cancer cell lines (11, 14). Conversely, UNBS1450 is able to induce autophagy-related cell death (14) and lysosomal membrane permeabilization in non-small cell lung cancer cells (11). Furthermore, induction of autophagy-related cell death is facilitated by ROS increases (a feature reported for UNBS1450 in this study; Fig. 2D)

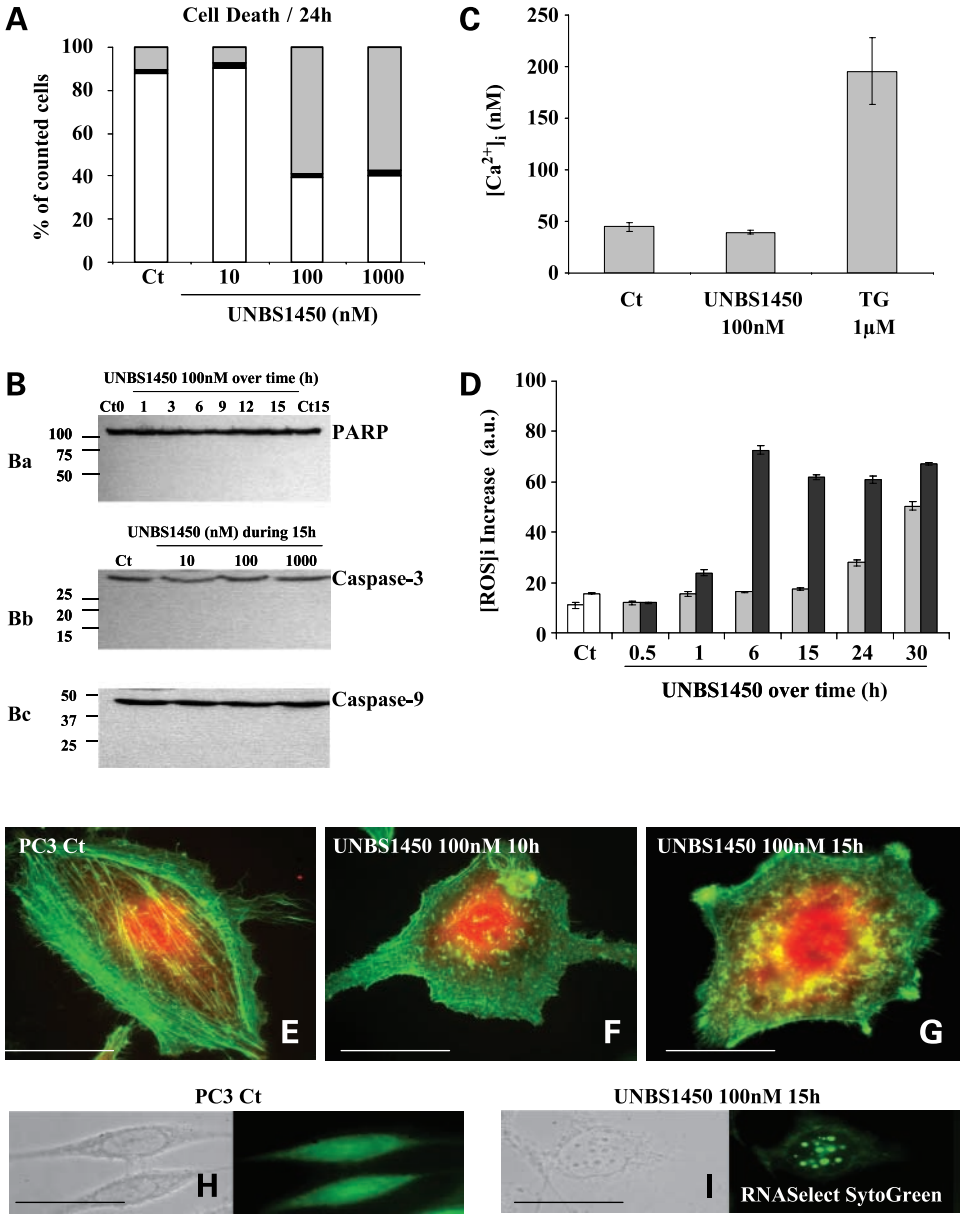

Figure 2. UNBS1450 causes a time- and dose-dependent increase in nonapoptotic-related PC-3 cell death. **A,** characterization of UNBS1450-induced effects with respect to the level of cell death (monitored by means of flow cytometry) over 24 h. *Open columns,* normal cells (Annexin V negative, propidium iodide negative), *black* and *gray columns,* apoptotic (Annexin V positive, propidium iodide negative) and possibly necrotic (Annexin V positive, propidium iodide positive) cells, respectively. **B,** effects of 100 nmol/L UNBS1450 over a period of 15 h on the cleavage pattern of poly (ADP-ribose) polymerase (*Ba*); intact (uncleaved) poly (ADP-ribose) polymerase has a molecular weight of 116 kDa. *Bb* and *Bc,* effects of UNBS1450 over a period of 15 h on the activation of caspase-3 and caspase-9, respectively. **C,** evaluation of the increase in $[Ca^{2+}]_i$ on UNBS1450 treatment at 100 nmol/L. A subsequent application of thapsigargin (*TG*), an inhibitor of SERCA pumps, increased $[Ca^{2+}]_i$, thus indicating that the treatment did not induce a release of total calcium from the reticulum. **D,** evaluation of the increase in ROS following UNBS1450 treatment at 10 nmol/L (*gray columns*) and 100 nmol/L (*black columns*). **E** to **G,** analysis of 100 nmol/L UNBS1450-mediated disorganization of the actin cytoskeleton after 10 h (**F**) and 15 h (**G**) of treatment in comparison with untreated PC-3 cells (**E**). Bar, 50 μm. **H** and **I,** observed nucleolar condensation may result from RNA accumulation in nucleoli as evidenced by nucleolar Syto Green RNA Select (Molecular Probes) staining pattern. *Left,* bright-field images; *right,* autofluorescence images. Bar, 150 μm.

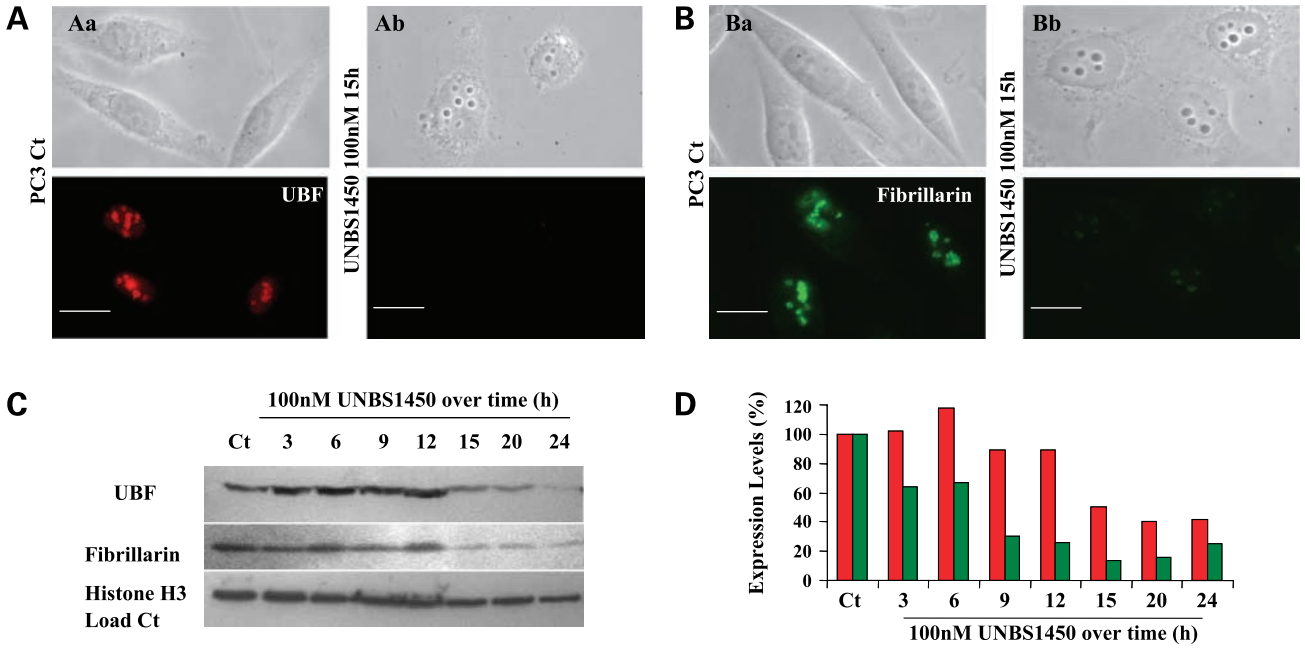

E UNBS1450 DOWN-REGULATED MESSENGERS FOR NUCLEOLAR PROTEINS

Symbol	Name	GeneBank	Score Ct/UNBS1450
UBTF	upstream binding transcription factor, RNA polymerase I	AU145147	2.02
DKC1	dyskerin	U59151	2.11
GNL3	guanine nucleotide binding protein-like 3 (nucleolar)	NM_014366	2.15
NOL7	nucleolar protein 7, 27kDa	AF130102	2.31
MKI67IP	MKI67 (FHA domain) interacting nucleolar phosphoprotein	AL577809	2.44
IMP3	IMP3, U3 small nucleolar ribonucleoprotein, homolog (yeast)	AL136913	2.47
NOL3	nucleolar protein 3 (apoptosis repressor with CARD domain)	AI912351	2.82
NOL8	nucleolar protein 8	NM_017948	2.94
UTP14A	UTP14, U3 small nucleolar ribonucleoprotein, homolog A (yeast)	BC001149	4.27

Figure 3. UNBS1450 impairs the organization of the nucleolus in PC-3 cells. Nucleolar morphology of untreated (*Aa* and *Ba*) and 100 nmol/L UNBS1450-treated (*Ab* and *Bb*) human prostate PC-3 cancer cells as observed with bright-field microscopy. UNBS1450 induced segregation of the nucleolar components as evidenced by means of UBF (**A**) and fibrillarin (**B**) immunofluorescence staining. *Bottom,* immunofluorescence images; *top,* corresponding bright-field images. Bar, 100 μm. **C,** effects of 100 nmol/L UNBS1450 treatment on UBF and fibrillarin protein expression as evidenced by means of Western blotting. Histone H3 was used as the loading control. **D,** quantification of 100 nmol/L UNBS1450-induced effects on UBF (*red columns*) and fibrillarin (*green columns*) protein expression presented in (**C**). The quantification was achieved with respect to loading control and presented as percentage of inhibition (the untreated control condition was set as 100%). **E,** table representing 100 nmol/L UNBS1450 down-regulated nucleolar proteins in PC-3 cells as revealed by means of genome-wide microarray analysis after 12-h incubation.

and nuclear factor-κB deactivation (a feature reported previously for non-small cell lung cancer; ref. 11).

Computer-assisted videomicroscopy (15, 16, 26) has enabled UNBS1450-induced anticancer effects to be directly visualized. This approach ruled out the hypothesis of UNBS1450-triggered cell death resulting from induction of osmotic shock, senescence, or mitotic catastrophe. Furthermore, this also revealed that UNBS1450 treatment induced major modifications in PC-3 cell and nucleus shape, including the enlargement of nuclei in treated cells. As indicated above, this enlargement is not a consequence of osmotic shock as ascertained using videomicroscopy or as a result of an increase in $[Ca^{2+}]_i$ (Fig. 2C) or $[Na^+]$ (14). Rather, it was observed that at 100 nmol/L UNBS1450 markedly impaired the dynamics of the actin cytoskeleton (13, 14). Figure 2E illustrates the morphologic pattern of the polymerized (green fluorescence) as opposed to the non-polymerized (globular; red fluorescence) actin cytoskeleton in PC-3 cells left untreated with respect to UNBS1450. In contrast, Fig. 2F and G (10 h and 15 h, respectively, in the presence of 100 nmol/L UNBS1450) reveal that the compound markedly impaired the dynamics of the actin cytoskeleton. In addition to disorganizing the actin cytoskeleton, UNBS1450 provoked striking effects on nucleolar morphology, including marked fractionation, compaction, and formation of dark enlargements (Figs. 2H and I, 3 and 4). The RNA Select Syto Green staining method further indicated that these changes were accompanied by accumulation of RNA in the nucleolus (Fig. 2H and I). The identification of actin in several nuclear complexes

implicates it in diverse nuclear activities, including transcription, chromatin remodeling, and nucleocytoplasmic trafficking (27). Thus, actin cytoskeleton disorganization may lead to unprocessed RNA accumulation in nucleoli and/or to transcribed RNA sequestration due to impaired nucleocytoplasmic trafficking.

UNBS1450 Leads to Marked Changes in Nucleolar Morphology

As evidenced in Fig. 2I and further sustained in Figs. 3 and 4, bright-field microscopy revealed striking effects of UNBS1450 on nucleolar morphology. Nucleolar assembly depends on the activation of RNA polymerase I transcription machinery, itself requiring at least two factors in addition to active polymerase I: the promoter selectivity factor (SL1; ref. 28) and the UBF (a key regulator of rRNA synthesis; ref. 29). UNBS1450 almost completely abolished UBF expression in PC-3 cells when used at 100 nmol/L for 15 h [as evidenced using immunofluorescence techniques (Fig. 3A) and this decline was largely substantiated in quantitative Western blots (Fig. 3C and D)]. UBF down-regulation therefore impairs rDNA transcription generating pre-rRNAs (47S in mammals), which recruit the rRNA-processing machinery (17) producing 18S, 5.8S, and 28S mature rRNAs (28). One of the first-acting rRNA maturation factors is fibrillarin. As shown in Fig. 3B to D, UNBS1450 also almost completely abolished fibrillarin expression in PC-3 cells when used at 100 nmol/L for 15 h as evidenced using immunofluorescence (Fig. 3B) and further confirmed by means of quantitative Western blots (Fig. 3C and D), therefore impairing nucleolar organization and possibly also rRNA processing. It is worth noting that ouabain, under the same experimental conditions, did not induce dark enlargement of PC-3 nucleoli or the down-regulation of fibrillarin expression (data not shown).

Additionally, using a genome-wide microarray approach, it was shown that treatment of PC-3 cells with 100 nmol/L UNBS1450 over 12 h resulted in down-regulation of at least nine nucleolar proteins, among which was UBF (Fig. 3E). UNBS1450 also mediated dyskerin down-regulation (Fig. 3E). Dyskerin is a nucleolar protein that carries out two separate functions, both fundamental to proliferating cells. One is the pseudo-uridylation of rRNA molecules,

A UNBS1450 DOWN-REGULATED MESSENGERS FOR MYC AND MYC-RELATED PROTEINS

Symbol	Name	GeneBank	Score Ct/UNBS1450
MYCPBP	c-myc promoter binding protein	BE268538	2.02
NMI	N-myc (and STAT) interactor	NM_004688	2.17
MAX	MYC associated factor X	BC003525	2.22
MINA	MYC inducednuclear antigen	AB083191	2.88
MYC	v-myc myelocytomatosis viral oncogene homolog (avi)	NM_002467	4.19

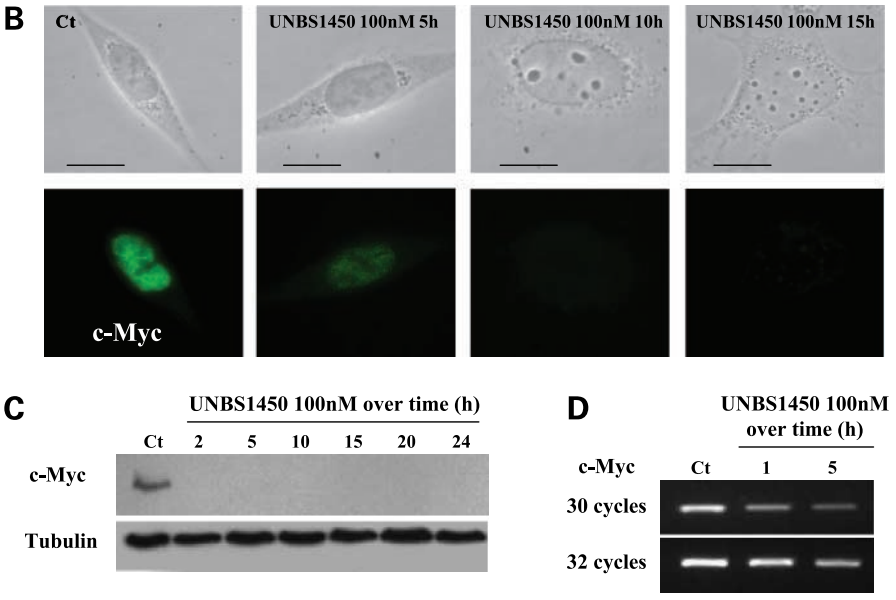

Figure 4. UNBS1450-induced down-regulation of c-Myc expression. **A,** table representing UNBS1450 down-regulated myc and myc-related genes as revealed by genome-wide microarray analysis. **B,** immunofluorescence analysis of c-Myc expression in untreated and 100 nmol/L UNBS1450-treated PC-3 cells for 5, 10, and 15 h. *Bottom,* immunofluorescence images; *top,* corresponding bright-field images. Bar, 100 μm. **C,** Western blotting analysis evidencing UNBS1450-induced down-regulation of c-Myc expression. Tubulin was used as the loading control. **D,** semiquantitative PCR analysis (with presented results for 30 and 32 cycles) for c-Myc RNA accumulation following 100 nmol/L UNBS1450 treatment over 1 and 5 h in comparison with untreated cells. All cDNA were used at the same concentration (20 ng).

necessary for their processing, and the other is the stabilization of the telomerase RNA component, necessary for telomerase activity (30). Dyskerin expression and function are associated with tumor progression. Additionally, patients with low expression have a better clinical outcome than those with high dyskerin levels (30). Its down-regulation may thus inhibit tumor proliferation. These results indicate that UNBS1450-induced nucleolar disorganization may result from its action on both major nucleolar constituents (UBF, fibrillarin, and dyskerin) and other proteins with nucleolar function.

UNBS1450-Induced Nucleolar Disorganization Seems to Be Mediated through c-Myc Down-Regulation in PC-3 Cells

Using the genome-wide microarray approach, it was also shown that PC-3 cell treatment with 100 nmol/L UNBS1450 over 12 h resulted in down-regulation of at least five Myc-related proteins, including c-Myc itself (Fig. 4A). This result was further confirmed by semiquantitative PCR analysis, which revealed a gradual decrease in accumulated c-Myc RNA after 100 nmol/L UNBS1450 treatment over 1 and 5 h (Fig. 4D). c-Myc is required for activating rDNA transcription in response to mitogenic signals and it coordinates the activity of all three nuclear RNA polymerases, thereby playing a key role in regulating ribosome biogenesis and cell growth (31, 32). Schlosser et al. (33) have also reported previously the identification of 38 c-Myc target genes with nucleolar function. It is interesting to note that among the nucleolar genes affected by UNBS1450 treatment, as reported in Fig. 3E, at least three are known to be regulated by c-Myc [UBF, dyskerin, and nucleolar phosphoprotein Nopp34 (MKI67IP)]. Figure 4B shows that UNBS1450 at 100 nmol/L almost completely abolished c-Myc expression in PC-3 cells after 15 h of exposure. These results obtained by immunofluorescence labeling were confirmed using Western blotting (Fig. 4C). UNBS1450-induced c-Myc down-regulation is a rapid phenomenon, as after only 2-h exposure to the compound no c-Myc could be

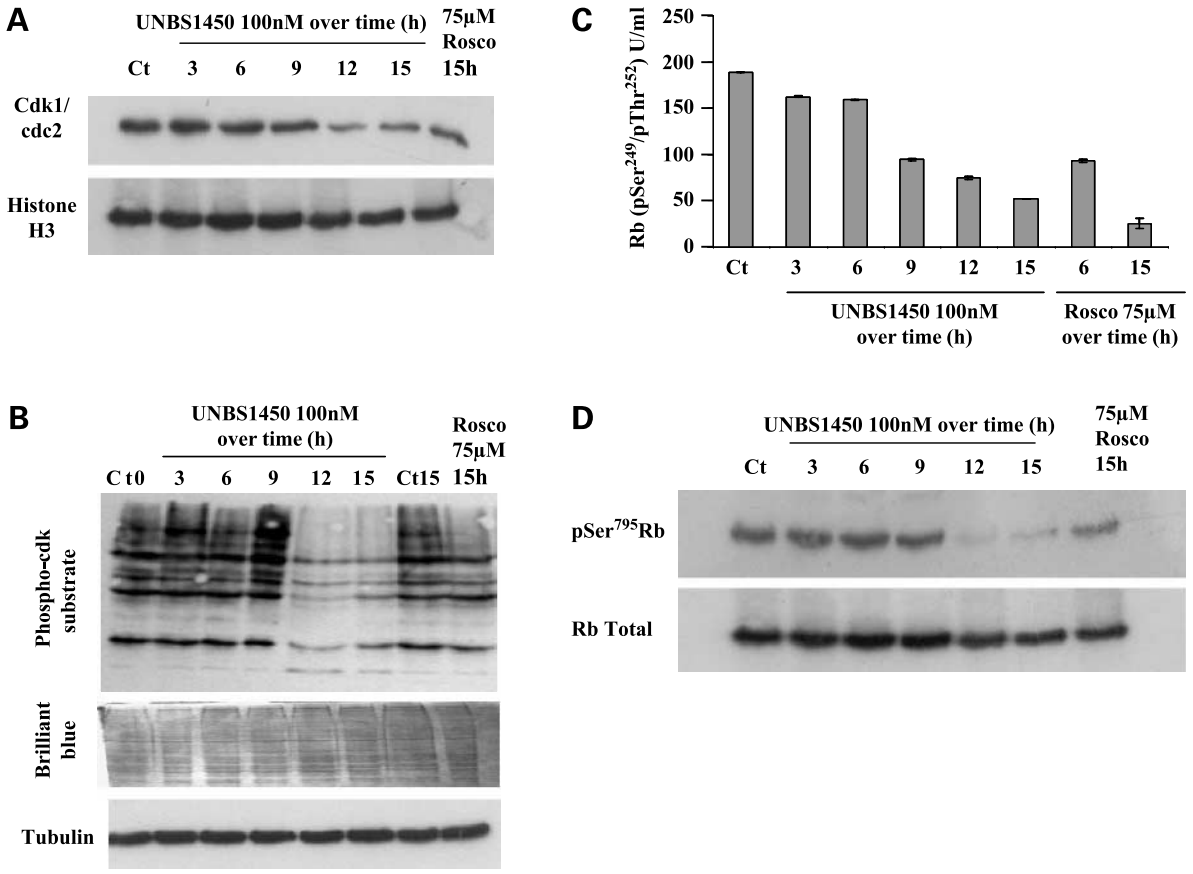

Figure 5. UNBS1450-mediated effects on CDK and Rb expression and activity. **A,** Western blotting analysis revealing UNBS1450-induced down-regulation of Cdk1 expression. Histone H3 was used as the loading control. **B,** Western blotting analysis revealing UNBS1450 inhibition of phosphorylation of CDK substrates. *Ct0,* control condition at the beginning of the experiment; *Ct15,* control condition at the end of the experiment (15 h). Brilliant blue staining and tubulin immunoblotting were used as protein quantity and quality controls. **C,** a phospho-Rb ELISA assay revealing that UNBS1450 inhibited phosphorylation of Rb protein, resulting from inhibition of CDK. Roscovitine (*Rosco*; a CDK inhibitor) was used at 75 µmol/L as a positive control. **D,** Western blotting analysis revealing UNBS1450-induced down-regulation of pSer^{795}Rb expression (*top*) and lack of effect on total Rb protein expression (*bottom*).

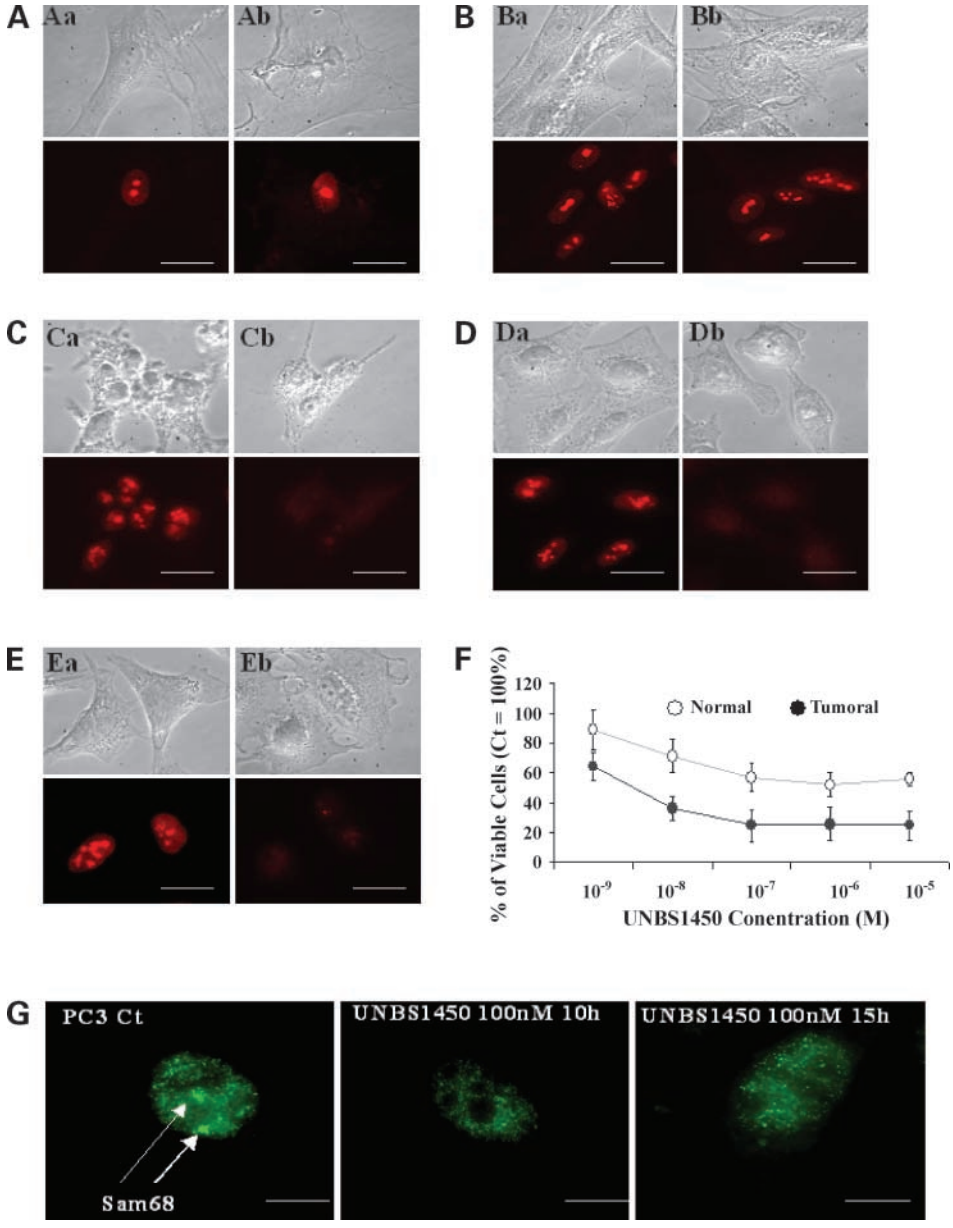

Figure 6. UNBS1450 selectively impairs nucleolus organization and function in human cancer cells compared with normal cells. **A** and **B,** UNBS1450 (1 μmol/L over 15 h) did not modify the organization of the nucleoli in normal human skin WS-1 (**A**) and lung WI-38 (**B**) fibroblasts as evidenced by means of bright-field microscopy and UBF staining. *Aa* and *Ba,* untreated cells; *Ab* and *Bb,* 1 μmol/L UNBS1450-treated cells. **C** to **E,** UNBS1450-induced (10 nmol/L over 15 h) disorganization of the nucleoli in human prostate cancer cells LNCaP (**C**), DU145 (**D**), and PC-3 (**E**) as evidenced by means of UBF staining. *Ca, Da,* and *Ea,* (untreated cells); *Cb, Db*, and *Eb,* 10 nmol/L UNBS1450-treated cells. Bar, 150 μm. **F,** UNBS1450-induced marked antiproliferative effects on human prostate LNCaP, DU145, and PC-3 cancer cell lines (*black line,* mean) compared with the effects on human normal WS-1 and WI-38 cells (*gray line,* mean). Mean ± SE. **G,** UNBS1450-induced disruption of the Sam68 body (Src-associated in mitosis 68 kDa) was evidenced using immunofluorescence staining for Sam68 protein. Bar, 50 μm.

evidenced by Western blotting (Fig. 4C). Thus, the reported UNBS1450-mediated antitumor effects involving nucleolar disorganization could also be the result, at least partly, of c-Myc down-regulation.

UNBS1450-Induced Nucleolar Disorganization Seems Also to Be Mediated through a Decrease in CDK Expression and Activity in PC-3 Cells

Nucleolar organization is also highly dependent on the CDK expression and activation status (28, 34). Several cyclins and CDKs, among which is CDK1, have been reported to be under c-Myc transcriptional control.[7] As shown in Fig. 5A, 100 nmol/L UNBS1450 markedly down-regulated CDK1 expression in treated PC-3 cells. In addition, using a Western blotting approach, it was determined that UNBS1450 very efficiently inhibited phosphorylation of CDK substrates in PC-3 cells (Fig. 4B). The effects observed with 100 nmol/L UNBS1450 after 12- to 15-h treatment of PC-3 cells (Fig. 5B) were more marked than those observed with 75 μmol/L roscovitine, a CDK inhibitor.

UNBS1450 Decreases the Levels of Phosphorylation of pRb in PC-3 Cells

Specific attention has also been given to the effects of UNBS1450 on the expression of phospho-Rb. This represents a dynamic manner to show that a compound modifies CDK

[7] http://www.myc-cancer-gene.org/site/mycTargetDB.asp

activity, as pRb activity is partly under the control of CDKs (35). An ELISA assay was used for the detection of the phosphorylated form of Rb ($pSer^{249}/pThr^{252}$) resulting, at least partly, from the action of CDKs (35). It was observed that UNBS1450 markedly decreased in a time-dependent manner the level of phospho-Rb expression in PC-3 cells, with a magnitude of effect at 100 nmol/L similar to that observed with roscovitine at 75 μmol/L (Fig. 4C). This result was reinforced by Western blotting analysis, which revealed a UNBS1450-induced decrease in the phosphorylation level of another Rb phosphorylation site (that is, Ser^{795}) without significant modification of total Rb protein expression (Fig. 5D).

All these data appear to indicate that, at least in part, UNBS1450-mediated nucleolar disorganization is mediated via down-regulation of c-Myc and CDK expression and their signaling pathways.

UNBS1450 Seems to Selectively Impair Nucleolus Organization and Function in Cancer Cells Compared with Normal Cells

As already indicated, bright-field microscopy revealed that UNBS1450 at 100 nmol/L did not modify the organization of nucleoli in normal human WS-1 and WI-38 fibroblasts (data not shown), whereas it markedly did so in human prostate cancer cell lines: DU145 (data not shown) and PC-3 (Figs. 3 and 4). The selectivity of the compound for cancer over normal cells is further shown in Fig. 6A to E. Indeed, even when used at 1 μmol/L, UNBS1450 did not affect UBF expression in normal cell lines: WS-1 and WI-38 fibroblasts when treated for 15 h (Fig. 6A and B) or 48 h (data not shown). However, 10 nmol/L UNBS1450 almost completely abolished UBF expression in androgen-dependent LNCaP (Fig. 6C) as well as androgen-independent prostate cancer cell lines DU145 (Fig. 6D) and PC-3 (Fig. 6E). Cardenolide-mediated antiproliferative selectivity toward cancer cells reported previously (reviewed in ref. 8) was also further confirmed in this study using the MTT assay for global cell growth (Fig. 6F).

The nucleolus could represent a selective target in cancer therapy because the nucleoli of cancer cells present several differences to those of normal cells. One difference concerns perinucleolar bodies in the shape of perinucleolar compartments and the Sam68 bodies (18). Sam68 nucleolar bodies consist of Sam68 protein, nucleolar proteins, and nucleic acids (18). As shown in Fig. 6G, UNBS1450 at 100 nmol/L disrupted the Sam68 nucleolar body.

Discussion

During the time cardiac glycosides have been used in cardiac disease, many reports have suggested their possible use in medical oncology (8). Furthermore, Johnson et al. (36), using cell-based high-throughput screening of chemical libraries against several potential cancer targets, found that a class of cardiac glycosides potently inhibited the plasma membrane sodium pump (Na^+/K^+-ATPase) resulting in the inhibition of four of six prostate cancer target genes. Additionally, several cardenolides have also shown significant antitumor activities in experimental cancer models (3–6, 10–14). The data from the present study indicate that the new cardenolide UNBS1450, a representative of a novel structural class, displays significant anticancer activity through an original mechanism of action, that is, nucleolar targeting.

The receptor of cardiac glycosides is the sodium pump, which represents a very interesting and potentially selective target in anticancer therapy because the expression levels of its various α and β subunits markedly differ in cancer compared with normal cells (8, 13, 14, 37, 38) and their distribution are also tissue type dependent (8, 9). The signaling pathways affected by cardenolides seem to be different in normal (proproliferative) and cancer cells (antiproliferative; reviewed in ref. 8). Thus, it is not surprising to evidence different cardenolide-mediated mechanisms of action in different cell types.

Using cellular imaging (15, 16, 26), it was observed that UNBS1450 markedly modifies nucleolus morphology in terms of nucleolar condensation and fragmentation. The nucleolus itself may be an interesting potential target in cancer therapy due to the observation that the nucleoli of cancer cells are characterized by the presence of perinucleolar bodies, like Sam 68, not found in normal cells (18). A recent publication from Busa et al. (39) indicates that Sam68 expression supports prostate cancer cell proliferation and survival to cytotoxic agents. This article reveals that Sam68 is frequently up-regulated in human prostate cancers and that down-regulation of its expression or activity affects prostate cancer cell proliferation and survival (39). As shown in Fig. 6G, UNBS1450 at 100 nmol/L disrupted the Sam68 nucleolar body. Furthermore, Paronetto et al. (40) reported that more advanced-stage prostate cancer patients are characterized by highly activated SRC kinases. These in turn phosphorylate Sam68 and this unregulated Sam68 phosphorylation might lead to nonregulated release and translation of mRNAs, altering the control of cell cycle and the proliferation of prostate cancer cells. In line with this, it is interesting to note that on investigation it was shown that 100 nmol/L UNBS1450 decreased the levels of Tyr^{418}-Src phosphorylation in PC-3 cells (data not shown), which might further favor Sam68 deactivation and Sam68 body disruption.

Furthermore, it should be borne in mind that the nucleolus appears to be a key player in nuclear functional architecture (41). Nucleolar organization could be affected by several factors, such as blockade of rDNA transcription, c-Myc expression, and CDK activation (28, 31, 33, 34). It is well established that blocking rDNA transcription induces nucleolar disassembly and segregation of nucleolar machinery (28), which is clearly evidenced with UNBS1450 at 100 nmol/L in PC-3 cells (Figs. 3 and 4). UBF is a key regulator of rRNA synthesis (the first event in ribosome biogenesis), owing to its ability to modulate RNA polymerase I transcriptional activity: (*a*) phosphorylation of UBF up-regulates rRNA synthesis in response to external stimuli and in neoplasia, (*b*) up-regulation of UBF activity has been shown to arise from direct extrastimulatory

stimuli, and (*c*) UBF can thus serve as a stimulus that might directly activate the translational machinery to initiate tumorigenesis (29).

c-Myc has also been shown to directly regulate ribosome biogenesis through the transcription of r-proteins and the regulation of S6K activity. The genes up-regulated in c-Myc-transfected cells consist of several essential nucleolar proteins such as fibrillarin, UBF, nucleoplasmin, and nucleolin (29, 33, 34, 42). These proteins function in the processing of rRNA precursors and have been implicated in the regulation of ribosome assembly or the nucleocytoplasmic transport of mature ribosomal subunits (29). In prostate cancer development c-Myc exerts an important role (1, 43). Experimental evidence shows that inhibiting c-Myc significantly halts tumor cell growth and proliferation (44). Indeed, inhibition of c-Myc expression by an antisense phosphorodiamidate morpholino oligomer is one of the new approaches being evaluated to treat prostate cancer (45). However, although several approaches aiming to inhibit c-Myc function are under evaluation (44, 46), to the best of our knowledge, no compound has been described as a potent inhibitor of c-Myc expression and thus a potent anticancer agent per se. The data from the present study reveal that UNBS1450, with already established antitumor properties *in vitro* and *in vivo*, almost completely abolished c-Myc expression in PC-3 cells. The marked UNBS1450-induced c-Myc down-regulation could result, at least partly, from rapid compound-induced increases in ROS. In fact, Chou et al. (47) showed that ROS can inhibit gene expression, in part by the oxidation of Sp1. Oxidized Sp1 loses DNA-binding activity and contributes to the suppression of several genes including c-Myc. Also, several reports reveal that c-Myc transcription is partly under STAT3 transcriptional control (48). Using genome-wide microarray analysis, we have been able to evidence UNBS1450-mediated down-regulation of STAT3 expression. It is worth noting that UNBS1450 c-Myc down-regulation (observed at both mRNA and protein levels) seems to be irreversible in contrast to small interfering RNA–mediated c-Myc down-regulation (data not shown). Western blot and immunofluorescence analyses further revealed that UNBS1450 provoked marked down-regulation of c-Myc expression even at 10 nmol/L in six of eight different human carcinoma cell lines evaluated, in contrast to none with ouabain, digoxin, and digitoxin.[8] These differences may be related to the structural specificity of UNBS1450. At 100 nmol/L, UNBS1450 almost completely abolished c-Myc expression in all tested carcinoma cells. This down-regulation in human carcinoma cells appears to be mediated via the interaction of UNBS1450 with the sodium pump $\alpha 1$ subunit, as no c-Myc down-regulation could be shown in rodent cancer cells,[8] which display cardenolide-insensitive $\alpha 1$ subunits because of a double mutation.

[8] Personal observations.

Nucleolar organization is also dependent on the CDK activation status (28, 34). Inhibition of CDKs in interphasic cells hampers correct pre-rRNA processing and induces a dramatic disorganization of the nucleolus. Sirri et al. (28) have proposed that the mechanisms governing both formation and maintenance of functional nucleoli involve CDK activities and couple the cell cycle to ribosome biogenesis. Also, several cyclins and CDKs, including CDK1, have been reported to be under c-Myc transcriptional control.[7] UNBS1450 has been found in this study to inhibit CDK activity in a more pronounced manner than roscovitine (Fig. 5), a CDK inhibitor (34). Therefore, this CDK inhibition, in addition to UNBS1450-induced c-Myc down-regulation, could be responsible for the severe nucleolar disorganization observed on UNBS1450 treatment of cancer cells.

It is important to emphasize that the effects resulting from the action of UNBS1450 are not due to a global inhibition of transcription. Indeed, using a genome-wide microarray approach, it was shown that the expression of 1798 genes was significantly affected (up- or down-regulated at least two-fold), of which 725 were up-regulated and the remaining 1,073 were down-regulated. Using EASE software for functional gene classification, the most affected cellular component was the nucleus and the most affected biological processes were RNA processing and regulation of transcription.

In conclusion, the data from the present study indicate that the structurally novel cardenolide UNBS1450 is characterized by a completely new mechanism of antitumor action. These UNBS1450-induced effects appear to relate to its capacity to promote actin cytoskeleton disorganization, as well as nucleolar structure disorganization and dysfunction, through ROS increase and by impairment of CDK and Myc expression and associated signaling pathways.

Disclosure of Potential Conflicts of Interest

T. Mijatovic and N. De Nève: Unibioscreen SA employees; R. Kiss: Unibioscreen SA former employee, presently a consultant and shareholder. The other authors reported no potential conflicts of interest.

References

1. Bernard D, Pourtier-Manzanedo A, Gil J, Beach DH. Myc confers androgen-independent prostate cancer cell growth. J Clin Invest 2003; 112:1724 – 31.

2. Jemal A, Siegel R, Ward E, Murray T, Xu J, Thun MJ. Cancer statistics, 2007. CA Cancer J Clin 2007;57:43 – 66.

3. Yeh JH, Huang WJ, Kan SF, Wang PS. Inhibitory effects of digitalis on the proliferation of androgen dependent and independent prostate cancer cells. J Urol 2001;166:1937 – 42.

4. McConkey DJ, Lin Y, Nutt LK, Ozel HZ, Newman RA. Cardiac glycosides stimulate Ca^{2+} increases and apoptosis in androgen-independent, metastatic human prostate adenocarcinoma cells. Cancer Res 2000; 60:3807 – 12.

5. Huang YT, Chueh SC, Teng CM, Guh JH. Investigation of ouabain-induced anticancer effect in human androgen-independent prostate cancer PC-3 cells. Biochem Pharmacol 2004;67:727 – 33.

6. Lin H, Juang JL, Wang PS. Involvement of Cdk5/p25 in digoxin-triggered prostate cancer cell apoptosis. J Biol Chem 2004;279:29302 – 7.

7. Xie Z, Askari A. Na^+/K^+-ATPase as a signal transducer. Eur J Biochem 2002;269:2434 – 9.

8. Mijatovic T, Van Quaquebeke E, Delest B, Debeir O, Darro F, Kiss R.

Cardiotonic steroids on the road to anti-cancer therapy. BBA Rev Cancer 2007;1776:32 – 57.

9. Blanco G. Na,K-ATPase subunit heterogeneity as a mechanism for tissue-specific ion regulation. Semin Nephrol 2005;25:292 – 303.

10. Van Quaquebeke E, Simon G, Andre A, et al. Identification of a novel cardenolide (2″-oxovoruscharin) from *Calotropis procera* and the hemisynthesis of novel derivatives displaying potent *in vitro* antitumor activities and high *in vivo* tolerance: structure-activity relationship analyses. J Med Chem 2005;48:849 – 56.

11. Mijatovic T, Mathieu V, Gaussin JF, et al. Cardenolide-induced lysosomal membrane permeabilization contributes therapeutic benefits in experimental human non-small-cell-lung cancers. Neoplasia 2006;8: 402 – 12.

12. Mijatovic T, Op De Beek A, Van Quaquebeke E, et al. The cardenolide UNBS1450 is able to deactivate NF-κB-mediated cytoprotective effects in human non-small-cell-lung cancer (NSCLC) cells. Mol Cancer Ther 2006;5: 391 – 9.

13. Mijatovic T, Roland I, Van Quaquebeke E, et al. The α1 subunit of the sodium pump could represent a novel target to combat non-small cell lung cancers. J Pathol 2007;212:170 – 9.

14. Lefranc F, Mijatovic T, Kondo Y, et al. Targeting the α1 subunit of the sodium pump (the Na^+/K^+-ATPase) to combat glioblastoma cells. Neurosurgery 2008;62:211 – 21.

15. Debeir O, Van Ham P, Kiss R, Decaestecker C. Tracking of migrating cells under phase-contrast video microscopy with combined mean-shift processes. IEEE Trans Med Imaging 2005;24:697 – 711.

16. Decaestecker C, Debeir O, Van Ham P, Kiss R. Can anti-migratory drugs be screened *in vitro*? A review of 2D and 3D assays for the quantitative analysis of cell migration. Med Res Rev 2007;2:149 – 76.

17. Hernandez-Verdun D, Roussel P, Gebrane-Younes J. Emerging concepts of nucleolar assembly. J Cell Sci 2002;115:2265 – 70.

18. Spector DL. Nuclear domains. J Cell Sci 2001;114:2891 – 3.

19. Zaidi SK, Young DW, Javed A, et al. Nuclear microenvironments in biological control and cancer. Nat Rev Cancer 2007;7:454 – 63.

20. R Development Core Team. R: a language and environment for statistical computing. Vienna (Austria): R Foundation for Statistical Computing; 2006.

21. Gentleman RC, Carey VJ, Bates DM, et al. Bioconductor: open software development for computational biology and bioinformatics. Genome Biol 2004;5:R80.

22. Wilson CL, Miller CJ. Simpleaffy: a BioConductor package for Affymetrix quality control and data analysis. Bioinformatics 2005;21: 3683 – 5.

23. Bolstad BM, Irizarry RA, Astrand M, Speed TP. A comparison of normalization methods for high density oligonucleotide array data based on variance and bias. Bioinformatics 2003;19:185 – 93.

24. Zhou X, Yin W, Doi SQ, Robinson SW, Takeyasu K, Fan X. Stimulation of Na,K-ATPase by low potassium requires reactive oxygen species. Am J Physiol Cell Physiol 2003;285:C319 – 26.

25. Newman RA, Yang P, Hittelman WN, et al. Oleandrin-mediated oxidative stress in human melanoma cells. J Exp Ther Oncol 2006;5: 167 – 81.

26. Lang P, Yeow K, Nichols A, Scheer A. Cellular imaging in drug discovery. Nat Rev Drug Discov 2006;5:343 – 56.

27. Bettinger B, Gilbert DM, Amberg DC. Actin up in the nucleus. Nat Rev Mol Cell Biol 2004;5:410 – 5.

28. Sirri V, Hernandez-Verdun D, Roussel P. Cyclin-dependent kinases govern formation and maintenance of the nucleolus. J Cell Biol 2002;156: 969 – 81.

29. Ruggero D, Pandolfi PP. Does the ribosome translate cancer? Nat Rev Cancer 2003;3:179 – 92.

30. Montanaro L, Brigotti M, Clohessy J, et al. Dyskerin expression influences the level of ribosomal RNA pseudo-uridylation and telomerase RNA component in human breast cancer. J Pathol 2006;210:10 – 8.

31. Arabi A, Wu S, Ridderstrale K, et al. c-Myc associates with ribosomal DNA and activates RNA polymerase I transcription. Nat Cell Biol 2005;7: 303 – 10.

32. Grandori C, Gomez-Roman N, Felton-Edkin ZA, et al. c-Myc binds to human ribosomal DNA and stimulates transcription of rRNA genes by RNA polymerase I. Nat Cell Biol 2005;7:311 – 8.

33. Schlosser I, Holzel M, Murnseer M, Burtscher H, Weidle UH, Eick D. A role for c-Myc in the regulation of ribosomal RNA processing. Nucleic Acids Res 2003;31:6148 – 56.

34. Wojciechowski J, Horky M, Gueorguiena M, Wesierska-Gadek J. Rapid onset of nucleolar disintegration preceding cell cycle arrest in roscovitine-induced apoptosis of human MCF-7 breast cancer cells. Int J Cancer 2003;106:486 – 95.

35. Coqueret O. Linking cyclins to transcriptional control. Gene 2002; 299:35 – 55.

36. Johnson PH, Walker RP, Jones SW, et al. Multiplex gene expression analysis for high-throughput drug discovery: screening and analysis of compounds affecting genes overexpressed in cancer cells. Mol Cancer Ther 2002;1:1293 – 304.

37. Espineda C, Seligson DB, Ball JW, Jr., et al. Analysis of the Na/K-ATPase α- and β-subunit expression profiles of bladder cancer using tissue microarrays. Cancer 2003;97:1859 – 68.

38. Rajasekaran SA, Ball WJ, Jr., Bander NH, Liu H, Pardee JD, Rajasekaran AK. Reduced expression of β-subunit of Na,K-ATPase in human clear-cell renal cell carcinoma. J Urol 1999;62:574 – 80.

39. Busa R, Paronetto MP, Farini D, et al. The RNA-binding protein Sam68 contributes to proliferation and survival of human prostate cancer cells. Oncogene 2007;26:4372 – 82.

40. Paronetto MP, Farini D, Sammarco I, et al. Expression of a truncated form of the c-Kit tyrosine kinase receptor and activation of Src kinase in human prostatic cancer. Am J Pathol 2004;164:1243 – 51.

41. Angelier N, Tramier M, Louvet E, et al. Tracking the interactions of rRNA processing proteins during nucleolar assembly in living cells. Mol Biol Cell 2005;16:2862 – 71.

42. Poortinga G, Hannan KM, Snelling H, et al. MAD1 and c-MYC regulate UBF and rDNA transcription during granulocyte differentiation. EMBO J 2004;23:3325 – 35.

43. Gil J, Kerai P, Lleonart M, et al. Immortalization of primary human prostate epithelial cells by c-myc. Cancer Res 2005;65:2179 – 85.

44. Ponzielli R, Katz S, Barsyte-Lovejoy D, Penn LZ. Cancer therapeutics: targeting the dark side of Myc. Eur J Cancer 2005;41:2485 – 501.

45. Devi GR, Beer TM, Corless CL, Arora V, Weller DL, Iversen PL. *In vivo* bioavailability and pharmacokinetics of a c-Myc antisense phosphorodiamidate morpholino oligomer, AVI-4126, in solid tumors. Clin Cancer Res 2005;11:3930 – 8.

46. Bidwell GL III, Raucher D. Application of thermally responsive polypeptides directed against c-Myc transcriptional function for cancer therapy. Mol Cancer Ther 2005;4:1076 – 85.

47. Chou WC, Chen HY, Yu SL, Cheng L, Yang PC, Dang CV. Arsenic suppresses gene expression in promyelocytic leukemia cells partly through Sp1 oxidation. Blood 2005;106:304 – 10.

48. Buettner R, Mora LB, Jove R. Activated STAT signaling in human tumors provides novel molecular targets for therapeutic intervention. Clin Cancer Res 2002;8:945 – 54.